UDC 629.78.533.6.013:621.45 https://doi.org/10.15407/itm2020.04.013

H. O. STRELNYKOV, O. L. TOKAREVA, O. D. IHNATIEV, N. S. PRYADKO, K. V.TERNOVA

INCREASING THE EFFICIENCY OF THE INTERCEPTOR THRUST VECTOR CONTROL SYSTEM OF ROCKET ENGINE

Institute of Technical Mechanics of the National Academy of Sciences of Ukraine and the State Space Agency of Ukraine,
Leshko-Popelya st., 15, 49005, Dnipro, Ukraine; e-mail: tokel@ukr.net

У даній роботі досліджуються статичні і динамічні характеристики газодинамічної (інтерцепторної) підсистеми комбінованої системи керування вектором тяги і визначаються шляхи підвищення її ефективності. Комбінована система керування включає в себе механічну і газодинамічну підсистеми. Газодинамічне регулювання вектора тяги є найбільш важливою і надійною підсистемою комбінованої системи керування.

Розглядається варіант збурення надзвукового потоку установкою твердої перешкоди (інтерцептору) в середній частині сопла ракетного двигуна. Важливою перевагою такого способу газодинамічного керування вектором тяги ракетного двигуна є практична відсутність втрат його питомого імпульсу на керування вектором тяги внаслідок відсутності витрати робочого тіла на створення керуючого зусилля. Інжекція через інтерцептори захищає його від впливу соплового надзвукового потоку і створює додаткове бічне зусилля.

До теперішнього часу не досліджено питання про оптимальне для створення керуючого зусилля місцезнаходження масопідводу по висоті інтерцептору і динамічні характеристики такої системи.

Мета роботи полягає в пошуку оптимального положення отвору масопідводу робочого тіла через інтерцептори для отримання максимальної добавки керуючого зусилля і визначенні впливу передавальних функцій елементів інтерцепторної системи на характеристики перехідного процесу при створенні керуючого зусилля.

При дослідженні статичних характеристик збурення надзвукового потоку газу в соплі інтерцептором зі вдувом через нього вторинного робочого тіла отримано практичний висновок про найбільш зручне розташування отвору вдуву у верхній частині інтерцептору з точки зору ефективності керування вектором тяги і захисту інтерцептору.

Отримано перехідну функцію процесу інтерцепторного регулювання напряму вектора тяги рідинного ракетного двигуна з урахуванням створення додаткового керуючого зусилля вприскуванням рідкого компонента палива. Встановлено, що втрата стійкості функціонування інтерцепторного вузла з вприскуванням залежить від перехідного процесу клапану, що регулює витрату робочого тіла на вприскування.

***Ключові слова**: ракетний двигун, система керування вектором тяги, статичні і динамічні характеристики, газодинамічна система, комбінована система керування.*

This work is concerned with studying the static and dynamic characteristics of the gas-dynamic (interceptor) subsystem of a combined system for thrust vector control and identifying ways to increase its efficiency. The combined control system includes a mechanical and a gas-dynamic subsystem. The gas-dynamic thrust vector control subsystem is the most important and reliable part of the combined control system.

Consideration is given to disturbing the supersonic flow by installing a solid obstacle (interceptor) in the middle part of the rocket engine nozzle. An important advantage of this method to gas-dynamically control the rocket engine thrust vector is that the thrust vector control loss of the specific impulse is nearly absent because the control force is produced without any consumption of the working medium. Injection through the interceptor protects it against exposure to the nozzle supersonic flow and produces an additional lateral force.

By now, the optimum height of the mass supply opening in the interceptor that maximizes the control force has not been determined, and the dynamic characteristics of this system have not been studied.

The aim of this work is to find the optimum position of the opening for working medium supply through the interceptor that maximizes the added control force and to determine the effect of the transfer functions of the interceptor system components on the characteristics of the control force production transient.

As a result of the study of the static characteristics of the supersonic flow disturbance in a nozzle with an interceptor through which a secondary working medium is injected, it is concluded that in terms of thrust vector control efficiency and interceptor protection the injection opening should be situated in the upper part of the interceptor.

The transfer function of interceptor control of the liquid-propellant rocket engine thrust vector is obtained with account for the production of an additional control force by the injection of a liquid propellant component. It is found that the loss of stability of the operation of an injection interceptor unit depends on the transient of the working medium injection control valve.

***Keywords**: rocket engine, thrust vector control system, static and dynamic characteristics, gas-dynamic system, combined control system.*

Introduction. A new concept of the thrust vector control system (TVCS) of a rocket engine (RE) – a combination of mechanical and gas-dynamic systems has been developed in the Institute of Technical Mechanics of the National Academy of Sciences of Ukraine and the State Space Agency of Ukraine It was substantiated [1] that such a system improves the efficiency and reliability of the flight control system of the rocket. The TVCS efficiency is increased due to the practical elimination of the RE specific impulse losses for thrust vector control and an increase in its dynamic characteristics. The reliability of the TVCS is increased due to the duplication of two subsystems control - mechanical (rotation of engine elements) and gas-dynamic (disturbance of the supersonic flow in the RE nozzle. The advantage of the mechanical subsystem is its simplicity and the practical absence of specific impulse losses for thrust vector control, possibility of creation nearly unlimited value of the required control force. The disadvantage is the need for powerful drives to provide the required dynamic characteristics of thrust vector control. The advantage of the gas-dynamic TVCS is its high dynamic characteristics, practical absence of specific impulse losses for thrust vector control and unlimited value of the required control force. The disadvantage is the need for powerful drives to provide the required dynamic characteristics of thrust vector control. In the combined TVCS, the advantages of these subsystems are realized due to their simultaneous operation and the disadvantages are eliminated due to the separation of the static and dynamic subsystem functions.

In this paper, the static and dynamic characteristics of the gas-dynamic (interceptor) subsystem are investigated and ways to increase its efficiency are determined. This subsystem is the most important in the combined thrust vector control system (KTVCS). If the mechanical subsystem of the TVCS fails, it provides the required control forces and high dynamic characteristics. At the same time the losses of the RE specific impulse can increase for creation possible large control forces.

Formal problem statement. Institute of Technical Mechanics of the National Academy of Sciences of Ukraine and the State Space Agency of Ukraine (ITM NASU & SSAU) has a lot of developed and patented variants of gas-dynamic system that are possible for solving various flight control problems. In this paper the disturbing of the supersonic flow by installing a solid obstacle (inceptor) in the middle part of the RE nozzle is considered. An important advantage of this method of gas-dynamic thrust vector control is absence of a working fluid consumption to create a control force. The disadvantage of the interceptor system is the instability (loss of operation) of the interceptor in the aggressive environment of the high-enthalpy flow of the nozzle gas running on it. The conditions are especially unfavorable for the operation of the inceptor in a two-phase free stream when the inceptor is exposed to the erosion effect of solid particles in the stream. Studies of similar thrust vector control systems [2] have shown ways to eliminate this drawback. In particular, it was shown that it is possible to ensure the operability of the inceptor by supply (injection) of a relatively cold working fluid through the inceptor. Secondary injection protects the inceptor from supersonic flow and creates additional lateral force.

Figure 1 shows the shadow pattern of the disturbed flow obtained in the experimental studies in ITM NASU & SSAU with gas (cold air) injection through the inceptor.

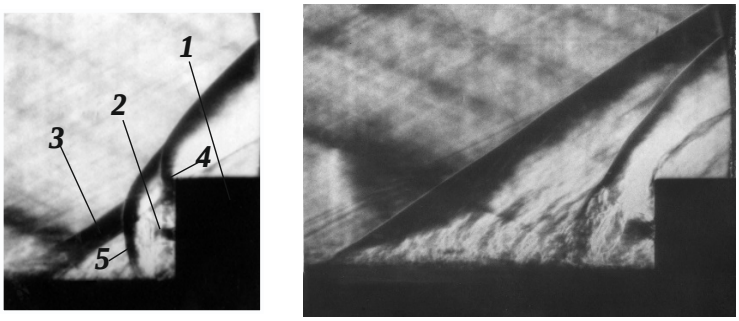

a) b)

1 – inceptor; 2 – gas jet injected from the inceptor; 3 – oblique shock wave initiating the boundary layer separation; 4 – head shock wave in front of the inceptor; 5 – head shock wave in front of the injected jet

Fig. 1 – A shadow picture of a supersonic flow perturbed by the inceptor on a flat wall with a minimum (a) and maximum (b) gas flow rate through the inceptor

When gas is blown upstream through the interceptor, the known a wave structure (including jumps 3 and 4 in Fig. 1, a)) in front of the obstacle in the supersonic flow is violated. At a low gas flow rate through the interceptor (Fig. 1, a)), an additional head shock wave 5 appears in front of the injected jet. At a high flow rate of the injected gas, the wave structure in front of the inceptor degenerates into one oblique shock. In the near-wall region, in front of the inceptor, a developed vortex structure with subsonic velocities is formed.

In studies [2], only qualitative results were obtained – the picture of the flow during gas injection through the inceptor in its middle (along the height) part. The injection influence on the efficiency of supersonic flow perturbing by interceptor has not been studied.

Literature review. The disturbance of a supersonic gas flow by an interceptor on the wall was studied in the seventies in the works of the Moscow State University, the Moscow Research Institute of Thermal Processes, and the ITM NASU & SSAU. Abroad, such works were carried out mainly in the United States.

Nowadays, in the Baltic State Technical University (St. Petersburg, Russia), numerical modeling of the flow disturbance in the rocket engine nozzle by asymmetric gas injection is being carried out. The study is simulated within the framework of the inviscid problem statement using various turbulence models [3 – 6]. Abroad, numerical investigations of asymmetric flow disturbances are carried out mainly in the USA [7 – 12].

However, nobody has investigated the question of the optimal (for creating a control force) location of the mass supply along the inceptor height. The dynamic characteristics of the inceptor system with a mass feeding through the inceptor have not been studied either.

The dynamic characteristic studies of the gas-dynamic TVCS carried out in the ITM showed that the dynamic system stability is one of the main factors that determine the control efficiency. At the same time, a significant influence of the dynamic parameters of the control transfer functions on the transition process stability is shown. The dynamics of the interceptor thrust vector control system with the injection of the working gas (fluid) through the inceptor has not been studied.

The aim of the work is to find the optimal position of the mass supply hole of the working gas through the inceptor to obtain the maximum addition of the control force and to determine the influence of the transfer functions of the interceptor system elements on the transient process characteristics at the control force creation

Materials of research. The interceptor is moved into the nozzle flow due to the pressure drop in the inceptor cavity and the pressure in the nozzle. The pressure in the interceptor cavity creates a working fluid (gas or liquid component) supplied through a controlled throttle of an electro hydraulic (or electropneumatic) valve. When the inceptor moves out of the nozzle wall into the oncoming supersonic flow of propellant combustion products, a disturbance arises in the flow with a positive excess static pressure, compared to the pressure of the undisturbed flow. The disturbance nature changes during injection working medium (gas or liquid) through the interceptor. In this case, the distribution of static pressure on the nozzle wall in the disturbed zone and the magnitude of the control force change. Injection through the inceptor also affects the dynamic characteristics of the entire gas-dynamic subsystem of the KTVCS. The studies of this work made it possible to establish new features of the disturbed flow in the nozzle during injection through the inceptor and to take into account the influence of the transfer functions of the interceptor subsystem elements on the characteristics of the transient process at control force creation. Below the results of the static and dynamic characteristic studying of the thrust vector control by the inceptor system are shown.

Static characteristics of the interceptor subsystem for RE thrust vector control. Determining the static characteristics of the TVCS requires determining the magnitude of the control force created when the inceptor is extended into the nozzle and a working fluid (gas or liquid) is injected through it. In this study, we considered the case of gas injection through a hole directed against the direction of the nozzle gas flow running on the inceptor. When a liquid is injected, a similar perturbation picture is observed, taking into account the liquid transformations (dusting and evaporation) in the high-temperature oncoming nozzle gas flow.

Numerical simulation of the disturbed flow is carried out with solving the Reynolds-averaged Navier-Stokes equations using the ANSYS FLUENT software package (SST-modification of the k - ω model).

A nozzle with the following characteristics was taken for the study. The nozzle contour is profiled along a streamline with a corner point. The radius of the nozzle throat is r_{cr} = 23.95 mm. The relative length of the supersonic part $\bar{L} = L / r_{cr}$ = 7.133. Geometric expansion ratio $\bar{r}_a = r_a / r_{cr}$ = 3.55. The average Mach number at the nozzle exit is M_a = 3,236. Total flow pressure in the nozzle p_0 = 6.717 MPa. Static pressure at the nozzle exit pa = 0.04 MPa. The stagnation temperature of the main flow in the nozzle is T_0 = 3458 K. Gas flow through the nozzle is G = 8.14 kg/s, thrust is R_y = 19.253 KN.

Further, the linear dimensions are related to the radius of the nozzle throat, area – to the throat area, pressure – to the total flow pressure in the nozzle, temperature – to the stagnation temperature of the main flow in the nozzle.

The interceptor has the following characteristics: diameter $\bar{d}_i$ = 0.292, height $\bar{h}_i$ = 0.376; distance from the minimum section $\bar{X}_i$ = 3.57; nozzle radius at the site of the inceptor installation $\bar{R}_n$ = 2.57; the relative area of the inceptor meridional

section $\overline{F_i}$ = 0.035; the angle of inclination of the nozzle wall (relative to the nozzle axis) at the site of the inceptor installation ~ = 19^0; injection hole area $\overline{F}$ = 0.00281; total pressure of injected gas $\overline{p}_{inj}$ = 0.6, stagnation temperature $\overline{T}_{inj}$ = 0.29; the height of the injection hole on the side inceptor surface from the nozzle wall relative to the inceptor height $\overline{h}_{inj}$ = 0.13, 0.5, 0.87.

The structured computational grid was built in the software package. The computational flow grid in the near-wall nozzle and inceptor regions, as well as in the boundary layer, was represented by layers of prismatic elements.

The lateral force magnitude is determined by the interceptor size and its location relative to the minimum nozzle section and the flow rate of the working fluid (in this case, gas) injected through the interceptor. In the numerical simulation of the disturbance in the nozzle, the inceptor was installed in the nozzle middle part perpendicular to the wall. The interceptor without injection and with gas injection against the direction of the main gas flow in the nozzle was considered.

The calculation results of the flow velocity vector distribution when the inceptor is extended without injection are shown in Fig. 2, a).

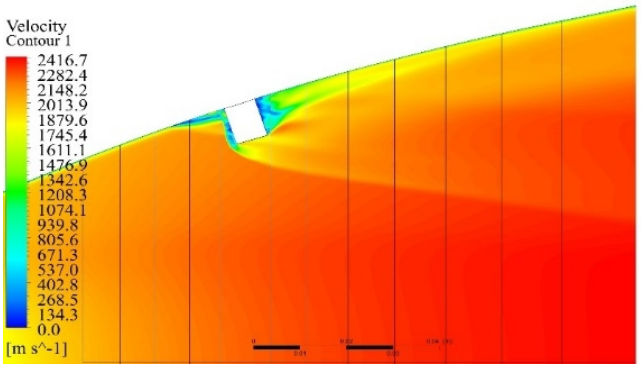

a)

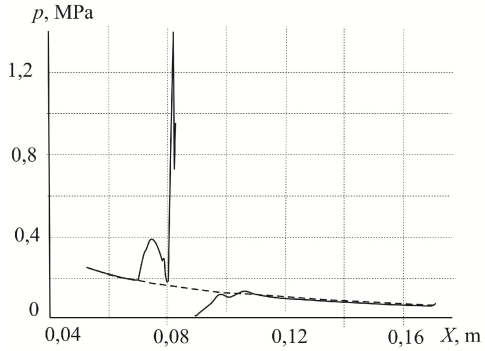

b)

a) distribution of the flow velocity vector;

b) distribution of static pressure on the nozzle wall

Fig. 2 – The supersonic flow disturbance in the nozzle by the inceptor without injection.

For flowing around the inceptor a – shaped shock wave system with an oblique shock is observed in front of the inceptor, causing separation of the boundary layer. This wave structure of the disturbed flow is fully consistent with

the structure obtained in experiments (see Fig. 1, a)). Flow disturbances extend downstream. The separation of the boundary layer in a supersonic flow leads to a redistribution of static pressure on the nozzle wall and the lateral force appearance. The distribution of static pressure on the nozzle wall is shown in Fig. 2, b)). The same flow structure was obtained in the experiments [2].The obtained calculated results, therefore, can be considered verified with experimental results.

Gas injection towards the incoming flow through the hole in the inceptor leads to a change in the flow pattern - wave structure, distribution of velocities and static pressure. In this case, depending on the injection hole height relative to the nozzle wall, the flow pattern changes significantly. The characteristics of the nozzle flow disturbance by the interceptor with injection at different positions of the injection hole are shown in Fig. 3 – 5. The dashed lines in the graphs Fig. 2 – 5 show the pressure distribution on the nozzle wall corresponding to the undisturbed flow.

Blowing through the inceptor in the immediate vicinity of the nozzle wall (Fig. 3, a)) leads to a change in the wave structure and the static pressure distribution compared to the case without blowing. A separation zone of the greatest length appears in front of the inceptor (in comparison with the cases of injection at a higher inceptor height).

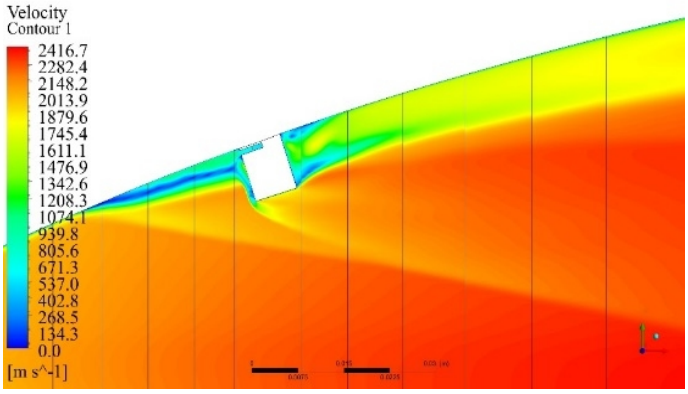

a)

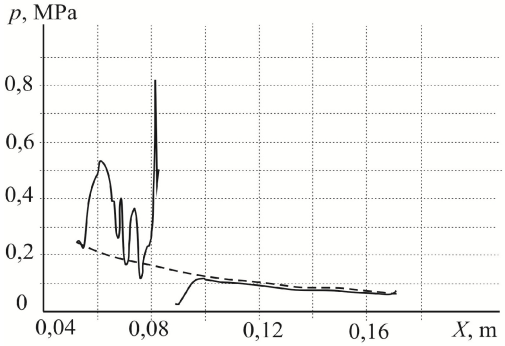

b)

a) – distribution of the flow velocity vector and

b) – distribution of static pressure on the nozzle wall at $\bar{h}_{inj}$ = 0,13 mm

Fig. 3 – Pictures of the nozzle flow, disturbed by the extension of the inceptor with injection

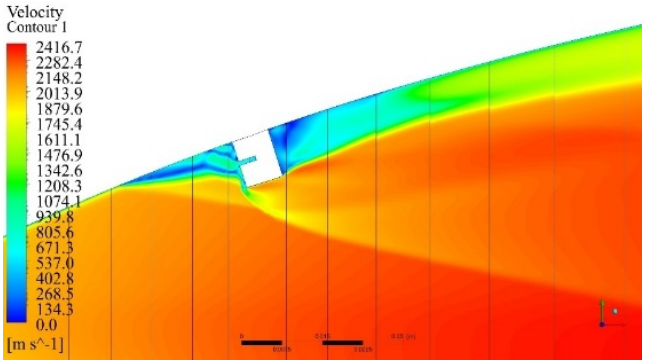

a)

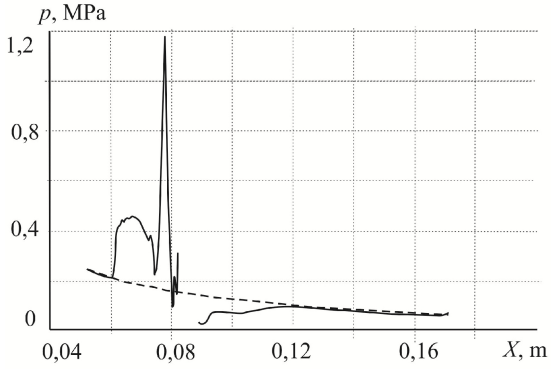

b)

a) – distribution of the flow velocity vector and

b) – distribution of static pressure on the nozzle wall at $\overline{h}_{inj}$ = 0,5 mm

Fig. 4 – Pictures of the nozzle flow, disturbed by the extension of the inceptor with injection

In this case, the excess pressure distribution in comparison with the pressure of the undisturbed flow (Fig. 3, b)) significantly differs from the known [2] universal distribution. During injection in the inceptor central part (along the height) a system of shock waves (Fig. 4, a)) with a head shock wave arises in front of the injected jet. In comparison with the injection near the nozzle wall (Fig. 3, a)), in this case, the running flow deflects the injected jet towards the nozzle wall. The excess pressure distribution in front of the inceptor takes the form of a universal one (Fig. 4, b)) - there are two maxima and two minima in the distribution. The first maximum is caused by the deviation of the running flow in the oblique shock wave, which caused the separation of the boundary layer. The second maximum is caused by a head shock wave in front of the inceptor. The minima in the distribution are caused by horseshoe-shaped vortex structures in the region disturbed by the inceptor. The reduced pressure area behind the interceptor (the separation zone of the incoming flow shaded by the inceptor) becomes more extended compared to the injection near the nozzle wall (see Fig. 3, b) and 4, b)).

Injection through the hole located in the upper part of the inceptor (Fig. 5, a)) leads to a greater moving of the head shock wave from the inceptor and, as a consequence, to extension the area of increased pressure in the whole separation zone, initiated by the inceptor moving into the supersonic flow. The excess pressure distribution in front of the inceptor is similar to the universal one (Fig. 5, b)).

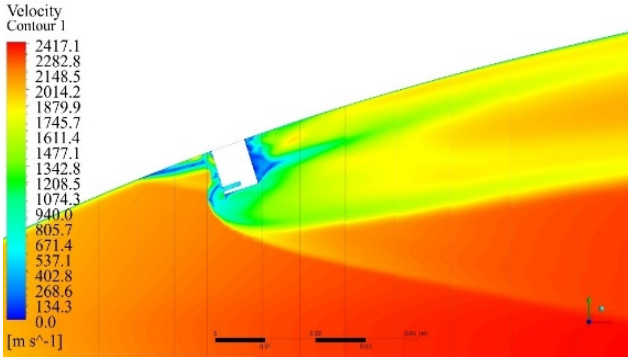

a)

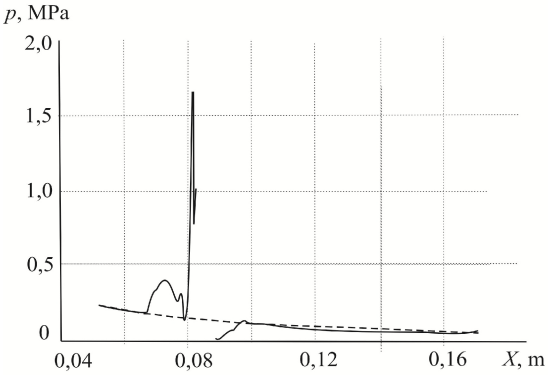

b)

a) – distribution of the flow velocity vector and

b) – distribution of static pressure on the nozzle wall at $\overline{h}_{inj}$ = 0,87 mm, respectively

Fig. 5 – Pictures of the nozzle flow, disturbed by the extension of the inceptor with injection

Thus, a change in the injection outlet (hole) position along the interceptor height significantly affects the disturbed flow nature in the flow running on the inceptor - its wave structure and the distribution of excess disturbed pressure. The picture of the disturbed flow during injection in the middle part of the inceptor corresponds to the picture obtained in experimental studies [2]. For injecting through the inceptor in the boundary layer region (near the wall streamlined by the incoming flow) the length of the front separation zone before the inceptor increases significantly and the distribution of excess perturbed pressure in front of the inceptor differs from the universal distribution adopted in the known studies of asymmetric supersonic flow disturbed by an obstacle on a streamlined wall. Two extreme cases of injection - near the nozzle wall and in the upper inceptor part show the possibility of increasing the injection efficiency. In the first case, it is due to an increase in the size of the zone disturbed by the obstacle on the streamlined wall. In the second case, it is due to an increase in excess pressure nearby in front of the inceptor (in the second maximum at the distribution of excess disturbed pressure). It should be noted that the farther the injection hole is located from the nozzle wall, the smaller the separation zone is in front of the inceptor and the reduced pressure zone behind it.

Studies of the injection inceptor hole location influence on the value of the control force made it possible to determine the preferred height of the injection

hole location along the inceptor height. The influence of the flow rate of the injected gas on the generated control force value was also investigated. The fig. 4 shows the dependences of the relative control force $\overline{R}_y$ (as a percentage of the nozzle thrust) on the relative height of the injection hole $\overline{h}_{inj}$ on the inceptor at different relative injection rates $\overline{G}_{inj}$. The injection hole height from the nozzle wall, is related to the height of the inceptor. The value of the lateral force at $\overline{h}_{inj} = 0$ corresponds to the inceptor without injection.

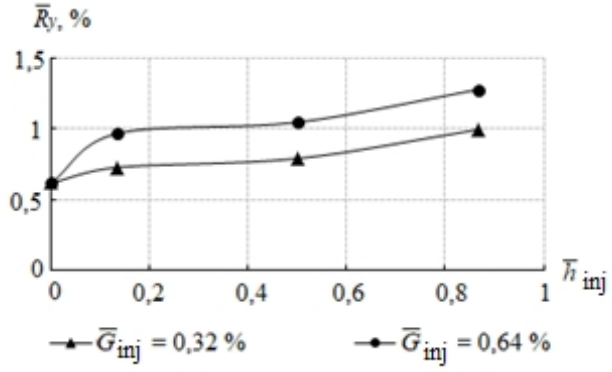

Fig. 4 – Lateral control force with interceptor regulation

As it can be seen from the graph, with an increase in the injection hole height (from the nozzle wall), the lateral force generated by the disturbance of the running on flow increases nonmonotonically. After a relatively sharp increase in lateral force efficiency with distance from the nozzle wall, it stabilizes when the hole is located in the middle part of the interceptor. With the approach of the injection hole to the top of the inceptor, the efficiency increases again. This is due to the reconfiguration of the wave gas flow structure in the nozzle zone disturbed by the inceptor. In this case, for other things being equal, a significant increase in the separation zone length in front of the inceptor, and hence the disturbance boundary of the running flow on in the case of injection near the nozzle wall, is less effective than increasing the maximum pressure in front of the inceptor in the case of injection in the upper part of the inceptor (with lower the size of the disturbed zone). This leads to a practical conclusion about the preferred injection hole location (from the point of view of the thrust vector control efficiency) – in the upper part of the inceptor. Besides, this injection hole location will also contribute to more effective protection of the inceptor from the erosion effect of the incoming supersonic flow due to the deflection by the incoming flow of the injected jet towards the nozzle wall, which contributes to more efficient inceptor washing with the injected flow.

Dynamic characteristics of interceptor control. Functional diagram of the combined thrust vector control system (KTVCS) with fixed drives of the mechanical subsystem is shown in Fig. 6.

The extension of the interceptor and injection through it can function autonomously; therefore, these processes are regulated by autonomous drives. In this case, the KTVCS is capable to solve the problems of missile stabilization and orientation. For this, in the functional diagram the parameter k_r is introduced, that characterizes the operation modes of the control system.

The control system signal $u_{cs} = u_{prog} - u_\theta$ is generated as a response to setting the programmed deflection angle u_{prog} ($k_r = 1$ – the rocket stage orientation mode) or an abnormal change in the deflection angle u_θ ($k_r = 0$ – the stage stabilization mode). Depending on the tasks, the control system (CS) distributes the signal to the interceptor drive u_{inj} and to the secondary injection drive u_i [13]. The voltage on each channel (hereinafter the designations without indices) generates an electric current i in the winding of an electromagnet inductor (on the EM diagram).

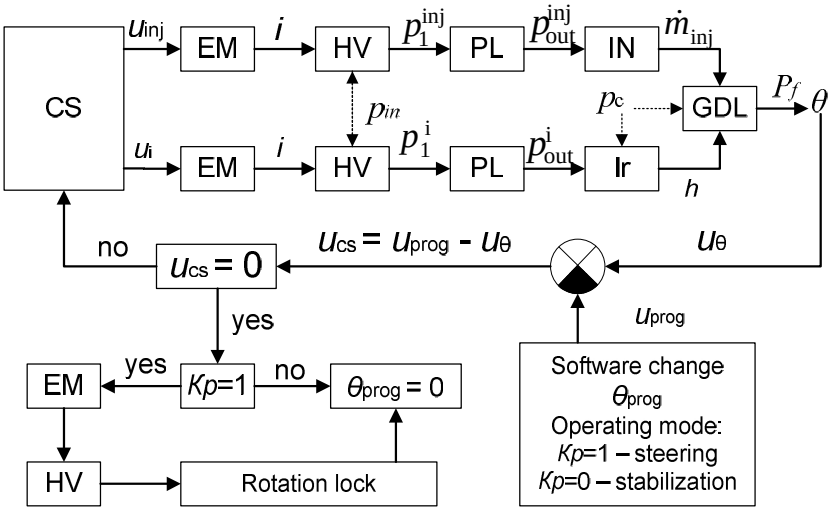

Fig. 6 – Functional diagram of the interceptor control of the thrust vector direction in the framework of the KTVCS with fixed drives of the mechanical subsystem

The electromotive force moves the armature of the electromagnet (EM), adjusting the parameters of the flow area of the hydraulic valve (HV). The flow rate of a component supplied through a short pipeline (PL) from an electrohydraulic valve (EHV) creates a pressure p^i under the action of which the interceptor (Ir) moved into the nozzle on the distance h. The obstacle created by the interceptor generates a lateral steering force. For injection through an interceptor channel – injection nozzle (IN), the working fluid flows $\dot{m}_{inj}$ with excess pressure p^{inj} into the supersonic part of the nozzle, generating additional lateral force P_f. The dependences of the lateral force on the parameters of the interceptor and secondary injection constitute the gas-dynamic link (GDL).

The injection and extension channels of the interceptor as part of the interceptor node operate in parallel. When the KTVCS is operating in the orientation mode upon the fact of the engine rotation (u_{cs}=0), a voltage pulse δ(t) is applied to the drive of the hinge lock, the space rocket stage (SRS) is rotated on the program angle $\bar{}_{pr}$. In the stabilization mode, the KTVCS is activated with the occurrence of abnormal disturbances in the SRS flight.

The dynamic characteristics of the interceptor control are based on a mathematical dynamic model the interceptor thrust vector control system with a liquid fuel component injection [14].

The block diagram of interceptor control with fuel component injection is shown in Fig. 7, where W_{EHV} is transient function of electrohydraulic valve (EHV), K_i (i = 1,..7) – coefficients of the gains of the transfer functions of the controls, T_4 – time constants of the transfer functions of the interceptor.

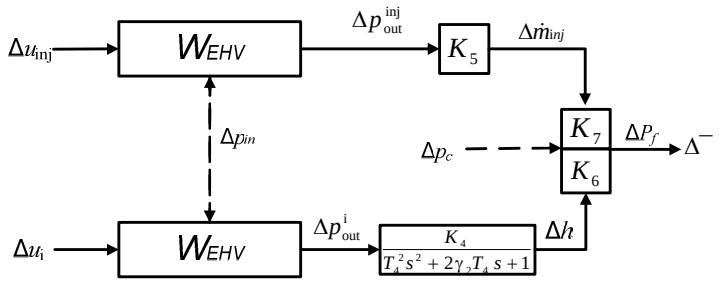

Fig. 7 – Block diagram of interceptor control with fuel component injection

The solid line in Fig. 7 shows the transformation sequence of the control input signal – the voltage supplied by the KTVCS to the interceptor extension drives and component injection regulators (the processes of signal passage are parallel). Dashed line is a sequence of signals for disturbances (pressures in the pressure main tube and on the wall of the nozzle supersonic part).

Fig. 8 shows a block diagram of the electro-hydraulic valve, which doses the fuel component supply.

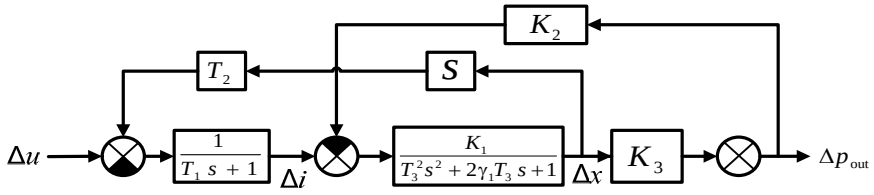

Fig. 8 – Block diagram of an electro-hydraulic valve

The dynamic parameters of the transfer functions presented below (time constants T_i and coefficients K_i) depend on the interceptor note design, normalizing factors and the working fluid parameters:

$$T_1 = \frac{L}{R},\ T_2 = \frac{k_{Px} x_{\text{nor}}}{R i_{\text{nor}}},\ T_3 = \sqrt{M_d \big/ \cdot},\ \text{¥}_1 = k_{vf} \big/ 2\sqrt{M_d \cdot},\ T_4 = \sqrt{M_i / c_i},$$

$$\text{¥}_2 = \frac{k_{df}}{2\sqrt{M_i c_i}},\ K_1 = k_{Pi} i_{\text{nor}} \big/ x_{\text{nor}} \cdot,\ K_2 = F_d\, p_{s\,\text{nor}} \big/ x_{\text{nor}} \cdot,\ K_3 = \frac{x_{\text{nor}}}{\dot{m}_{\text{nor}}} k_{mx},$$

$$K_4 = F_i \frac{p_{out\,\text{nor}}^{\text{i}}}{h_{\text{nor}} c_i},\ K_5 = \frac{1}{2} \frac{p_{out\,\text{nor}}^{\text{inj}}}{p_{out\,\text{nor}}^{\text{inj}} - p_{\text{c nor}}},$$

where L – is the electromagnet winding inductance; R – is the ohmic resistance of the control winding circuit; i – amperage; M_d – reduced mass of the moving parts of the EHV; k_{vf} – coefficient of viscous friction of the EGK working fluid; k_{Pi} – load characteristic of the electromagnet for the control current; k_{Px} – load characteristic of the electromagnet for moving the armature; x –course of the interceptor; k_{mx} – load characteristic of the shut-off element of the flow regulator; $\cdot = k_{Pi} + s_d - \frac{P_{hd\,\text{nor}}}{x_{\text{nor}}}$ – a parameter reflecting the relationship between the coefficient of dependence of the hydrodynamic force P_{hd} on the displacement of the

throttling device ("hydrodynamic stiffness") and the stiffness of the return spring s_d ("statism" of the regulator); F_d – the averaged value of the cross-sectional area of the EHV shut-off and regulating body, $\dot{m}$ – consumption of the working fluid through the throttle; M_i – the mass of the interceptor moving parts, taking into account the mass of the working body in the internal cavities; h – interceptor's step; c_i – spring rate of interceptor; k_{df} – coefficient of dry friction of the moving parts of the interceptor valve; p_s – supplied pressure to regulating bodies EGK; p_{out}^{i}, p_{out}^{inj} – supplied pressure to the interceptor and interceptor respectively; p_c – pressure in the engine nozzle at the installation site of the interceptor unit.

The subscript "nor" corresponds to the normalized values of the variable quantities. The superscript "inj" corresponds to the injection subsystem of the working fluid through the interceptor, "i" - to the interceptor subsystem.

Dynamic parameters $K_7=f(p_{out}^{i})$ and $K_8=f(p_{out}^{inj})$ are determined on the basis of dependencies obtained in the study of static characteristics and experimental data.

The control signals for the interceptor u_i and the injection u_{inj} pass sequentially through the inertial dynamic link corresponding to the electromagnetic drive and the oscillating link corresponding to the hydraulic valve (Fig. 8). The rest of the links along the injection channel are non-inertial. Along the extending interceptor channel, the control signal passes through the oscillating link corresponding to the interceptor valve (Fig. 7).

With the help of numerical calculations, the dynamic parameter values are calculated based on the nominal characteristics of real propulsion systems, the properties of real working bodies, the features of physical processes inside the interceptor unit and experimental data [2].

The initial characteristic parameter values for calculating the dynamic characteristics of the interceptor system with injection through the interceptor are given in the table.

M_i	F_i	c_i	k_{df}	h_{nor}	L	R	i_{nor}	k_{Pi}
2 кг	$6\cdot10^{-4}$ м2	150 Н/м	5 кг/с	0,1 м	1,4 Гн	54 Ом	0,5 А	1

k_{Px}	p_s	M_d	k_{vf}	k_{mx}	·	F_d	x_{nor}
1	$2\cdot10^{5}$ Па	0,1 кг	$1\cdot10^{-4}$ кг/с	1,5 кг/с^2	100 Н/м	$7\cdot10^{-4}$ м2	0,03 м

The frequency method is used to study the dynamic characteristics. This step makes it possible to analyze transient processes without finding the eigenvalues and eigenfunctions of differential equations. The frequency transient analysis method is based on the use of frequency characteristics, which can be determined from the transfer function of the system. The transfer function of the control system is a fractional rational function with respect to the Laplace variable $s = \omega j$, where ω is the signal frequency. For interceptor control of the thrust vector without taking into account the injection, the fraction numerator of the complex transfer function is a first-order polynomial, the denominator is a sixth-order polynomial. Taking into account injection, the numerator is a seventh order polynomial and the denominator is a tenth order polynomial.

The frequency characteristics of the interceptor unit are calculated using the MATLAB software package. The state of a dynamic system is assessed based on the analysis of its transient process.

In the mode when the working fluid injection is used to create an additional control force, numerical studies of the interceptor system dynamics have shown that the transient process is stable under a certain condition. The stability condition is that the EHV oscillatory link, which regulates the flow rate of the injected component, corresponds to an inertial (second order) transient process ($\gamma_1 > 1$). The same stability condition corresponds to the regime when the the working fluid injection is used only for cooling the interceptor [14].

At this stage of the research, it is assumed that EHV with the same characteristics control the interceptor and the injection moving. The influence of the load characteristics of autonomous EHV on transient process along the interceptor moving channel and along the injection channel are not considered.

The Fig. 9 shows the transient process graphs of the interceptor control, taking into account the additional control force creation by means of injection through the interceptor (solid line) and without it (dashed line).

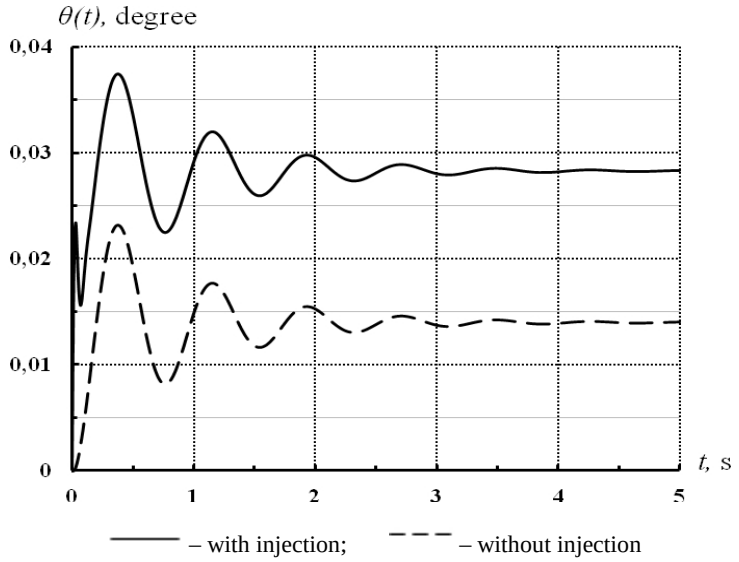

Fig. 9 – Transient process of interceptor regulation with injection

As it's seen from the graph, the injection creates an additional initial impulse of the lateral force, increasing the oscillation amplitude and not changing the transient process nature. At the same time, the transient process establishing time does not increase.

At calculations, it was found that the dry friction coefficient value (sliding friction) inside the interceptor valve affects significantly on the transient process. Taking into account the friction coefficient values for metals in vacuum, the transfer functions are calculated and transients are constructed for interceptor control taking into account injection (Fig. 10) at values of 5 kg/s (solid line), 8 kg/s (dotted line) and 12 kg/s (dashed line).

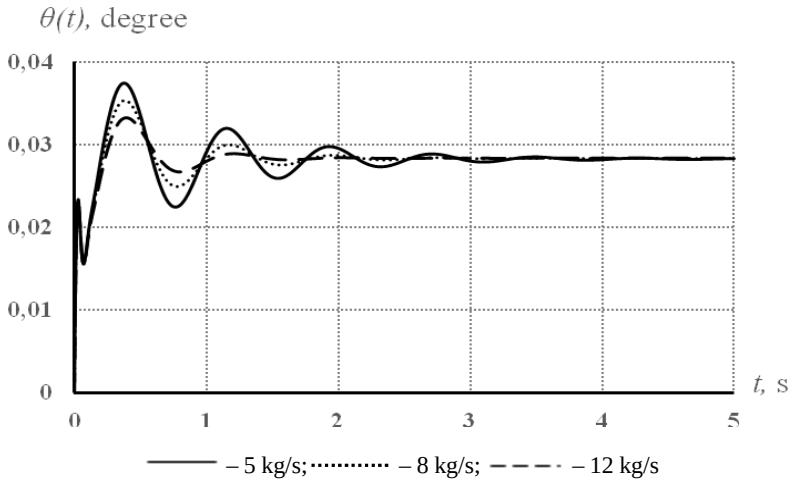

Fig. 10 – Transient process of interceptor regulation with injection at different friction coefficient values

With an increase in the friction coefficient, the transient process improves. The settling time and the vibration amplitude are reduced. However, an increase in the friction coefficient entails an increase in the return spring rigidity of the interceptor valve and an increase in the pressure in the pipeline leading the component to the interceptor.

The pressure value influence in the supply pipeline on the transient process can be estimated by comparing the transient functions in Fig. 11. The solid line corresponds to the pressure p_{out} = 2.5 atm, the small dashed line – 5 atm, the large dashed – 1,5 atm.

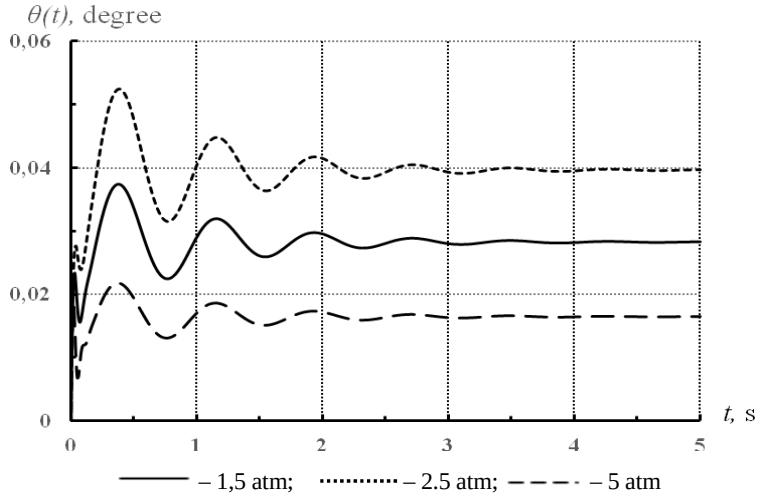

Fig. 11 – Transient process of interceptor regulation at different pressures in the supply line

An increase in pressure in the supply line decreases the steady-state value of the output signal, reduces the oscillation amplitude and insignificantly decreases the settling time, its degree of damping and the number of oscillations. The overshoot value is constant and amounts to 80 % of the set value.

The influence of the interceptor valve return spring stiffness on the transient process can be estimated from the graphs shown in Fig. 12. The solid line corre-

sponds to the stiffness c_i = 150 N/m, the small dashed line – 50 N/m, the large dashed line – 250 N/m.

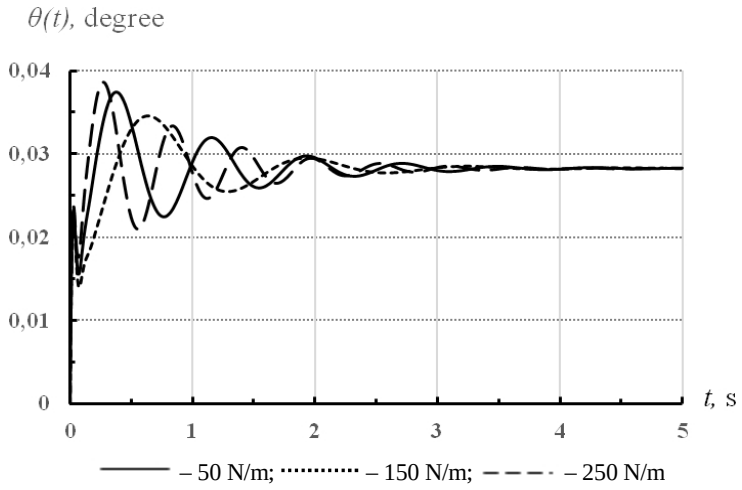

Fig. 12 – The interceptor regulation transient process at different spring rate values of the interceptor valve

With an increase in the return spring rigidity in the interceptor valve design, the vibration frequency increases. The amount of overshoot, the transient process duration and its attenuation degree do not change significantly.

The above calculation results show that there is a gain in the transient process quality and the output signal settling time due to the high friction coefficient of metal surfaces inside the interceptor valve (Fig. 10). In addition, it does not entail deterioration of the transient process from an increase in the pressure supplied to the valve (Fig. 11) and from an increase in the interceptor return spring rigidity (Fig. 12). In the engine design, an increase in the pressure supplied to the interceptor unit can lead to an increase in the power of the EHV and an increase in the return spring stiffness can increase the interceptor valve mass at mechanical spring using and increase the gas inlet power for the gas spring. The choice of the optimal (from the point of view of the transient process stability and the requirements for the energy and mass engine characteristics) characteristic parameters values of the interceptor regulation control bodies, which determine the dynamic parameters of its transfer function, remains the subject of further research.

Conclusions. In the study of the disturbance static characteristics of a supersonic gas flow in the nozzle by an interceptor with a secondary working fluid (gas) injected through it, a practical conclusion was obtained about the preferred (according to the efficiency of thrust vector control and protection of the interceptor) injection hole location in the upper interceptor part. The transition process function of interceptor control of the thrust vector direction of a liquid-propellant rocket engine is obtained, taking into account the additional control force creation by the liquid propellant component injection. It is shown that the stability loss in the interceptor unit operation with injection depends on the valve transient process that regulates the flow rate of the working fluid. Dependences of the transient process on the initial data have been established, that allow improving the transient process

1. *Kovalenko N.D., Sheptun U. D., Kovalenko T. A., Strelnikov G. A.* The new concept of thrust vector control for rocket engine. System Technology. 2017. № 6 (107). P. 120–127.

2. *Kovalenko N. D.* Rocket engine as an executive body of the missile flight control system. Dnepro: Institute of Technical Mechanics of NAS and SSA of Ukraine. 2004. 412 p.
3. *Volkov K. N.* Flow structure and thrust change during gas injection into the supersonic part of the nozzle. Technical Physics Journal. 2019. Vol. 89, No. 3. P 353–359 https://doi.org/10.1134/S1063784219030265
4. *Volkov K. N., Emelyanov V. N., Yakovchuk M. S.* Multiparameter optimization of thrust vector controls based on the injection of a gas jet into the supersonic part of the nozzle. Computational methods and programming. 2018. Vol. 19, No. 2. P. 158–172.
5. *Volkov K. N., Emelyanov V. N., Yakovchuk M. S.* Numerical modeling of the interaction of a transverse jet with a supersonic flow using various turbulence models. Applied Mechanics and Technical Physics. 2015. Vol. 56, No. 5. P. 64–75. https://doi.org/10.1134/S0021894415050053
6. *Volkov K. N., Emelyanov V. N., Yakovchuk M. S.* Cross injection of a jet from the surface of a flat plate into a supersonic flow. Engineering Physics Journal. 2017. Vol. 90, No. 6. P. 1512–1517. https://doi.org/10.1007/s10891-017-1703-x
7. *EREem E., Albayrak K., Tinaztepe H. T.* Parametric study of secondary gas injection into a conical rocket nozzle for thrust vectoring. AIAA Paper. 2006. N 2006−4942. https://doi.org/10.2514/6.2006-4942
8. *Huang W., Liu W. D., Li S. B., Xia Z. X., Liu J., Wang Z. G.* Influences of the turbulence model and the slot width on the transverse slot injection flow field in supersonic flows. Acta Astronautica. 2012. Vol. 73. P. 1−9. https://doi.org/10.1016/j.actaastro.2011.12.003
9. *Huang W., Wang Z. G., Wu J. P., Li S. B.* Numerical prediction on the interaction between the incident shock wave and the transverse slot injection in supersonic flows. Aerospace Science and Technology. 2013. Vol. 28. No 1. P. 91−99. https://doi.org/10.1016/j.ast.2012.10.007
10. *Prince R. L., Rejith P., Balu R.* Numerical simulation of a hot gas injection thrust vector control system performance. Procedia Engineering. 2012. Vol. 38. P. 1745−1749. https://doi.org/10.1016/j.proeng.2012.06.212
11. *Kawai S., Lele S. K.* Mechanisms of Jet Mixing in a Supersonic Crossflow: A Study Using Large-Eddy Simulation. AIAA Paper. No. 2008-4575. July 2008. https://doi.org/10.2514/6.2008-4575
12. *Peterson, D.M., Candler, G.V.* Hybrid RANS/LES of a Supersonic Combustor. AIAA Paper. No. 2008-6923. Aug. 2008. https://doi.org/10.2514/6.2008-6923
13. *Strelnikov G. A., Tokareva E. L., Pryadko N. S., Ihnatiev A. D.* To the development of a structural diagram of a bifunctional control system for the thrust vector of a rocket engine. Technical mechanics.2018. No. 4. P. 57–67. https://doi.org/10.15407/itm2018.04.057
14. *Tokareva E. L., Pryadko N. S., Ternovaya E. V.* Dynamic characteristics of the combined control system of the rocket engine thrust vector. Technical mechanics. 2019. No. 3. P. 16–29.

Received on 21.10.2020,
in final form on 01.12.2020